Learning Effective Intrinsic Features to Boost 3D-Based Face Recognition

Chenghua Xu[1], Tieniu Tan[1], Stan Li[1],
Yunhong Wang[2], and Cheng Zhong[1]

[1] Center for Biometrics and Security Research (CBSR)
& National Laboratory of Pattern Recognition (NLPR),
Institute of Automation, Chinese Academy of Sciences, Beijing, China
{chxu, tnt, szli, czhong}@nlpr.ia.ac.cn
http://www.cbsr.ia.ac.cn/
http://nlpr-web.ia.ac.cn/English/irds/index.html
[2] School of Computer Science and Engineering, Beihang University, Beijing, China
yhwang@buaa.edu.cn

Abstract. 3D image data provide several advantages than 2D data for face recognition and overcome many problems with 2D intensity images based methods. In this paper, we propose a novel approach to 3D-based face recognition. First, a novel representation, called **intrinsic features**, is presented to encode local 3D shapes. It describes complementary non-relational features to provide an *intrinsic representation* of faces. This representation is extracted after alignment, and is invariant to translation, rotation and scale. Without reduction, tens of thousands of intrinsic features can be produced for a face, but not all of them are useful and equally important. Therefore, in the second part of the work, we introduce a **learning** method for learning most effective local features and combining them into a strong classifier using an AdaBoost learning procedure. Experimental results are performed on a large 3D face database obtained with complex illumination, pose and expression variations. The results demonstrate that the proposed approach produces consistently better results than existing methods.

1 Introduction

Biometric identification has received much attention recent years. Face is among the most common and most accessible modality. Over the past decades, most work has been focusing on 2D images [1]. Since 2D-based face recognition suffers from variations in pose, expression, and illumination, it is still difficult to develop a robust automatic face recognition system using 2D images.

With the rapid development of 3D acquisition equipment, 3D capture is becoming easier and faster, and face recognition based on 3D information is attracting more and more attention. The existing methods mainly focus on three categories: 3D to 3D, 2D aided by 3D, and 2D combined with 3D. 3D to 3D means that the gallery and the probe examples are both 3D data, such as range images, and feature extraction and representation are both in 3D space. 2D aided

A. Leonardis, H. Bischof, and A. Pinz (Eds.): ECCV 2006, Part II, LNCS 3952, pp. 416–427, 2006.

by 3D means that 2D face recognition is done with the assistant of 3D model [9, 12]. 3D model is explored to overcome the pose, expression and illustration variations in 2D recognition. 3D combined with 2D means that features are extracted from both 3D images and 2D color or intensity images [13, 14, 15]. This paper mainly pays attention to the first category and summarizes the existing methods as follows.

Regarding feature representation, research has been focused mainly on how to extract and represent 3D features. Some earlier methods on curvature analysis [2, 3, 4] have been proposed for face recognition based on high-quality range data from laser scanners. In addition, recognition schemes based on 3D surface features have been developed. Chua et al. [5] treat face recognition as a 3D non-rigid surface matching problem and divide the human face into rigid and non-rigid regions. The rigid parts are represented by point signatures to identify an individual. They have obtained a good result in a small database (6 persons). Beumier et al. [6] propose two methods of surface matching and central/lateral profiles to compare two instances. Both of them construct some central and lateral profiles to represent an individual, and obtain the matching value by minimizing the distance of the profiles. Tanaka et al. [7] treat the face recognition problem as a 3D shape recognition problem of rigid free-form surfaces. Each face is represented as an Extended Gaussian Image, constructed by mapping principal curvatures and their directions. In more recent work, Hesher et al. [8] use a 3D scanner for generating range images and registering them by aligning salient facial features. PCA approaches are explored to reduce the dimensionality of feature vector. Lu et al. [11] use the hybrid ICP algorithm to align the reference model and the scanned data, and adopt the registration error to distinguish the different people.

Despite of the efforts mentioned above, a number of problems remain to be solved for 3D face recognition:

- Only local features have so far been used to represent unary properties of individual points. These ignore relationships between points in a reasonably large neighborhood while such relationships may play important roles in object recognition.
- These local features have been so far considered independent of each other for different points. However, they are not so in practice.
- Because these features are correlated, sophisticated and even nonlinear. Methods are needed for constructing good classifiers. The current research in 3D face recognition has not looked into this challenge.

In this work, we attempt to address the above issues. The main contributions of this paper are as follows:

- We propose a novel feature, called associative features, based on Gaussian-Hermite moments [20], to encode relationships between neighboring mesh nodes. They are combined with complementary non-relational features to provide an *intrinsic representation* of faces.
- The resulting intrinsic features are likely to be correlated for nearby nodes, and an individual face may have non-convex manifold in the features space.

We introduce a learning mechanism to deal with the problems. AdaBoost learning [22] is adopted to select most effective features and to combine these features to construct a strong classifier. This provides a new way to improve the performance of 3D face recognition.

For testing the proposed approach, we collect a large 3D face databases. The proposed approach is shown to yield consistently better results than existing methods including the benchmarking PCA methods [8, 14], the point signature based methods [5] and the curvature based method [2, 3, 4].

The rest of this paper is organized as follows. Section 2 describes associative features and the resulting intrinsic feature representation used in this work. Section 3 describes the use of AdaBoost learning for feature selection and classifier construction. Section 4 reports the experimental results and gives some comparisons with existing methods. Finally, Section 5 summarizes this paper.

2 Intrinsic Feature Representation

A vector of intrinsic features is a concatenation of scattered features and associative features. They are extracted after preprocessing.

2.1 Preprocessing

Our preprocessing includes three steps, namely, nose tip detection, alignment and meshing. We aim to exactly align the range images and approximate the original range image with a simple and regular mesh, which prepares for the feature extraction and representation.

In the facial range data, the nose is the most distinct feature. We have proposed a robust method to localize the nose tip, which is described in detail in [18]. According to the experiments in our database, the correct detection rate is over 99%. Aided by the detected nose and the classic method of the Iterative Closest Point (ICP) [21], alignment is done by our previous method [17]. We select a front 3D image as the fixed model, and all the other 3D images are rotated and translated to align with it.

The original images usually consist of considerable dense and irregular points in 3D space. It is very difficult to efficiently extract the corresponding features. Here a simple and regular mesh approximates the original range images by the multi-resolution fitting scheme. The meshing procedure is shown in Fig.1. During meshing, we only regulate the Z coordinate of each mesh node, which not only speeds up the meshing process but also keeps the correspondences of the generated meshes. In this paper, we use a mesh with 545 nodes and 1024 triangles to balance the resolution of the facial mesh and the cost of time and space. This constructed mesh is of great benefit to feature representation and extraction.

All these meshes have the same pose and corresponding nodes, which have the same position in an X-Y plane and different values along a Z-axis. Thus a vector of *depth features* can then be formed as follows

$$D = \{Z(v_1), Z(v_2), \cdots, Z(v_n)\} \tag{1}$$

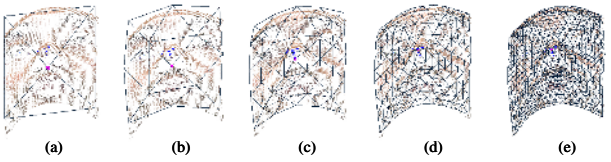

Fig. 1. The fitted meshes of different levels. (a) Basic mesh. (b)-(e) Level one to four.

where $Z(v_i)$ is the Z-coordinate of the mesh node v_i. They can be directly used for characterizing faces.

2.2 Cosine Signature Features

Here, we define a new metric, called *cosine signature* as a descriptor of local shape of each mesh node, as illustrated in Fig.2. Since a mesh well approximates the range image, we can obtain the following local information of each mesh node, p_e, that is, its spatial direct neighboring triangles, $\{T_1, T_2, \cdots, T_n\}$, its normal, N_{pe} and neighboring points in the range image within a small sphere. Due to the regularity of our mesh, the number of neighboring triangles of the common node (not the edge node) is usually six. The initial radius of the local sphere to decide the neighboring points is set as half of the length of one mesh edge in our work.

Further, the neighboring points can be classified into n categories, $\{C_1, \cdots, C_n\}$. Which category one point belongs to depends on which triangle the point's projection falls in the same direction as the normal, N_{pe}. For each class C_k, we can define its surface signal as follows:

$$d_{ek} = \frac{1}{2} + \frac{1}{2m} \sum_{i=1}^{m} cos(q_{ki} - p_e, N_{pe}) \tag{2}$$

with

$$cos(q_{ki} - p_e, N_{pe}) = \frac{(q_{ki} - p_e) \cdot N_{pe}}{\parallel q_{ki} - p_e \parallel \cdot \parallel N_{pe} \parallel} \tag{3}$$

where q_{ki} is the neighboring point belonging to class C_k, m is the number of points in C_k, and $d_{ek} \in [0, 1]$.

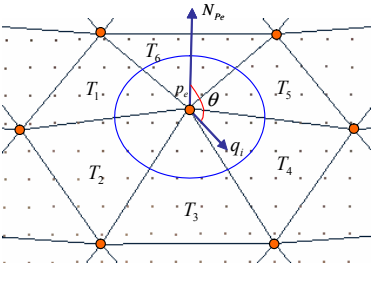

Fig. 2. Cosine signature of one mesh node

Then we can describe the local shape of each mesh node using the following vector:

$$s_e = \{d_{e1}, d_{e2}, \cdots, d_{en}\} \tag{4}$$

where d_{ek} is the surface signal. This vector describes the shape near this node, and we call it as *cosine signature*.

According to this metric, we can describe the shape of each row in the mesh with a combination of cosine signature of all nodes in this row respectively.

$$S_i = \{s_{i1}, s_{i2}, \cdots, s_{ir}\} \tag{5}$$

where S_i is the shape vector of the ith row and s_{ij} is the cosine signature of the jth vertex in the ith row. Further, from S_1 to S_n, we connect them in turn to form a long shape vector, S, in the alternate way of head and tail connection. The vector, S, is used to describe the shape of one face.

2.3 Associative Features

In the above, neither depth features or cosine signature features encode relationships in neighboring mesh nodes. In the following, we use Gaussian-Hermite moments (G-H moments) [20] to describe derivative or relational property of a local shape in a neighborhood, as a richer representation. Because such features describe the relational property of neighboring mesh nodes, we call it *associative features*.

It is well-known that moments have been widely used in pattern recognition and image processing, especially in various shape-based applications. More recently, the orthogonal moment based method has been an active research topic in shape analysis. Here, Gaussian-Hermite moments (G-H moments) are used for feature representation due to their mathematical orthogonality and effectiveness for characterizing local details of the signal [20]. They provide an effective way to quantify the signal variation. The nth order G-H moment $M_n(x, S(x))$ of a signal $S(x)$ is defined as [20]:

$$M_n(x) = \int_{-\infty}^{\infty} B_n(t) S(x+t) dt \quad n = 0, 1, 2, \cdots \tag{6}$$

with

$$\begin{aligned} Bn(t) &= g(t, \sigma) H_n(t/\sigma) \\ H_n(t) &= (-1)^n exp(t^2) \frac{d^n exp(-t^2)}{dt^n} \\ g(t, \sigma) &= (2\pi\sigma^2)^{-1/2} exp(-x^2/2\sigma^2) \end{aligned} \tag{7}$$

where $g(t, \sigma)$ is a Gaussian function and $H_n(t)$ is a scaled Hermite polynomial function of order n. G-H moments have many desirable properties such as insensitiveness to noise generated during differential operations.

In fact, the face surface is smooth on the whole, and high order moments usually describe the intense variation. So it is not necessary to calculate higher

order moments. In our experiments, we use the 0th-2nd order G-H moment with $\sigma = 2.0$ to represent the associative features.

To the constructed shape vector in the above, S, we calculate its nth order G-H moments, thus obtaining moment vectors, SM_n, which are called nth order associative features. They describe the relational property of neighboring mesh nodes.

2.4 Intrinsic Feature Vector

A vector of intrinsic features is a concatenation of scattered features and associative features. In our work, the scattered features include depth features, D (545 dimensions), and cosine signature, S (2814 dimensions). Associative features consist of 0th-2th order moments of cosine signature features, i.e., SM_n (2814 dimensions, n=0,1,2). The total dimension of intrinsic features is 11,801. These features represent not only the non-relational features but also the relationships between the neighboring mesh nodes. They provide a complete information to reveal the intrinsic property of facial surface. Their complementarity is effective to improve recognition accuracy, which will be further proved in the following experiments. In addition, since all these features are extracted after fine alignment, they are invariant to translation, scale and rotation.

3 Feature Selection and Classification

There are a total number of 11,801 such intrinsic features for a face image. They are likely to be correlated for nearby nodes, and an individual face may have non-convex manifold in the features space. In this work, AdaBoost learning algorithm with the cascade structure [22] is used for selecting most effective features and combining them to construct a strong classification.

The AdaBoost algorithm essentially works for a two-class classification problem. While face recognition is a multi-class problem, we convert it into one of two classes using the representation of intra-personal vs. extra-personal classes, following [23]. The intra-personal examples are obtained by using difference of images of the same person whereas the extra-personal examples are obtained by using difference of images of the different persons.

After this preparation, the AdaBoost-based learning procedure in [22] is used to learn a cascade of strong classifiers with N layers, each of which contains one or multiple weak classifiers.

During recognition stage, for one given probe sample, the different with each gallery example forms the vector, x. To each vector, x, the ith layer of the strong classifier returns the similarity measure, S_i. The larger this similarity value, the more this sample belongs to the intra-personal space. If $S_i < 0$, this layer rejects the sample. According to the multiple classifiers, we can obtain its total similarity:

$$S = \sum_{i=1}^{L} S_i \tag{8}$$

where L is the number of layers and S_i is the similarity of the ith layer. Thus we can obtain its similarity with each gallery example. Then the nearest neighbor scheme is used to decide which class the test sample belongs to.

In our training set, there are 23 persons and 33 images each person, and thus we obtain 12,144 positive examples and 275,517 negative examples. Every face image is represented as a vector of 11,801-dimensional intrinsic features, as explained above. Using the above learning procedure, we obtain a cascade of 20 classifiers with a total of 193 features.

4 Experiments

In this section, we demonstrate the excellent performance of our proposed scheme by comparing experiments in the terms of different features, different schemes and different combinations.

4.1 Databases

A large 3D face database has been collected to test the proposed algorithm. It was collected indoors during August and September 2004 using a non-contact 3D digitizer, Minolta VIVID 910, working on Fast Mode. This database contains 123 subjects, with each subject having 37 (without glasses) or 38 (with glasses) images. During the data collection, we consider not only separate variation of expressions, poses and illumination, but also combined variations of expressions under different lighting and poses under different expressions.

For the following experiments, images with large facial pose (80-90 degrees) and with glasses are excluded. The reasons are the following: (1) Our focus here is to compare different algorithms with images of approximate front faces whereas side view face recognition is too challenging for any methods. (2) The range scan quality was bad at glasses areas. Therefore, the actual database contains a total of 4059 images.

The database of 4059 images is divided into three subsets, that is, the training set, the gallery set and the probe set. The last 23 of the 123 subjects are used as the training set. The first images of the other 100 subjects (under the condition of front view, office lighting, and neutral expression) are used as the gallery set. The other images of the 100 subjects are used as the probe set.

There are 3200 images in the probe set. They are further divided into seven subsets:

- IV (400 images): illumination variations.
- EV (500 images): expression variations, including smile, laugh, anger, surprise and eye closed.
- EVI (500 images): expression variations under right lighting.
- PVS (700 images): small pose variations, views of front, left/right 20-30 degrees, up/down 20-30 degrees and tilt left/right 20-30 degrees.
- PVL (200 images): large pose variations, views of left/right 50-60 degrees.
- PVSS (700 images): small pose variations under smile.
- PVSL (200 images): large pose variations under smile.

4.2 Experiments with Different Features

In this experiment, we test the recognition performance using the different features. The considered features include surface curvature (SC) [2, 3, 4], point signature (PS) [5], COSMOS shape index (CO) [10, 11] and three kinds of features used in this paper, that is, depth features (DEP), cosine signature (COS) and associative features (ASS).

In our experiment, after the regular mesh is constructed following the schemes in Section 2.1, the different features are extracted for each node to characterize an individual. Then, we use one simple classifier to test the recognition performance, that is, PCA for reducing dimension and Euclidian distance for similarity measure. Table 1 shows the rank-one recognition accuracy (CCR, Correct Classification Rate) in different probe sets. In this table, the best recognition accuracy is emphasized. Fig.3 shows CMS (Cumulative Match Score) curves in the EV probe set.

From these result, we can obtain the following conclusion. (1) On the whole, the three features that we used have better performance than the other three; (2) In the probe sets related to expression and illumination variations, the

Table 1. CCR(%) using different features in the different probe sets (100 persons)

Probe sets	SC	PS	Co	DEP	COS	ASS
IV	97.6	87.0	89.0	98.5	**99.0**	**99.0**
EV	71.9	66.0	53.3	85.0	81.4	**85.2**
EVI	74.6	65.9	56.6	85.0	86.4	**87.0**
PVS	79.1	61.2	67.1	**85.1**	83.0	84.7
PVL	51.6	38.2	41.1	**70.0**	51.0	51.5
PVSS	63.7	53.3	44.5	**81.9**	75.4	76.9
PVSL	47.2	34.6	26.8	**65.0**	43.0	46.5

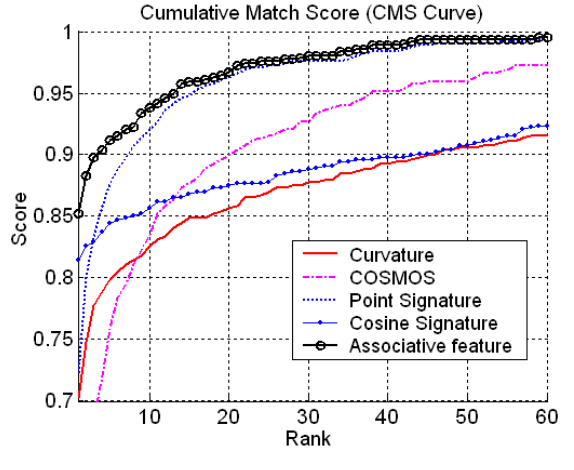

Fig. 3. CMS curves using different features in the EV probe set

proposed associative feature are more robust than depth information. This may be reasonably explained by the following reason. Depth information using the absolute range value is prone to shape variation, such as expression, whereas associative features use the relative information between reference nodes. These results also encourage us to improve the recognition performance by combining these complementary information.

4.3 Experiments with Different Schemes

In this section, we will test the different performances when using different classification methods, i.e., fusion scheme and AdaBoost learning.

Scattered features and associative features are of the different properties. Fusion rules [16] and AdaBoost learning [22] are two kinds of method to combine them. We test their performance by experiments. Using depth features, cosine signature and associative features, we construct the three single classifiers, respectively. After obtaining the matching score from each single classifier, the weighted sum rule [14] is used to combine them. The first row in Table 2 shows the rank-one recognition accuracy. In other way, from the intrinsic features consisting of scattered features and associative features, one cascade classifier is built following the scheme in Section 3. The CCR is shown in the second row in Table 2.

Table 2. CCR(%) of the different test sets in our face database (100 persons)

Probe sets	IV	EV	EVI	PVS	PVL	PVSS	PVSL
Fusion	99.5	88.0	90.2	96.1	73.5	**88.3**	67.5
AdaBoost	99.5	90.8	90.6	96.7	76.5	**87.9**	70.0

Comparing this result with Table 1, we can see that the recognition accuracy is better when combining the different features using the fusion scheme or AdaBoost learning. This verifies the conclusion in the last section.

From this result of Table 2, we also see that AdaBoost learning outperforms the fusion rule in all probe sets except the PVSS set. Further, we test the verification performance when using these two methods. Compared with single classifiers, the classifier by AdaBoost learning largely decreases the EER (Equal Error Rate) in all the probe sets. However, the classifier using the fusion scheme decreases the EER weakly. Fig.4 shows the ROC curves using single classifiers, fusion rule and AdaBoost learning in the EV probe set. On the whole, AdaBoost learning distinctly outperforms the fusion scheme.

4.4 Experiments with Different Combination

In [14], they evaluate the recognition performances of different combination of 2D and 3D images and draw the conclusion that multi-modal 2D+3D has the best performance. Their conclusion is very limited since they only explore the depth

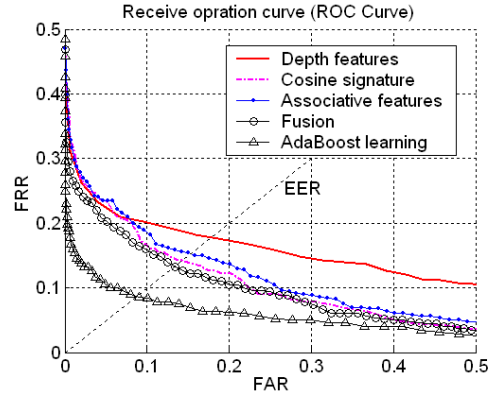

Fig. 4. ROC curves using single classifiers, fusion scheme and AdaBoost learning in the EV Probe set

Table 3. Rank-one recognition accuracy (%) with different combination (100 persons)

Probe sets	IV	EV	EVI	PVS	PVL	PVSS	PVSL
Depth+ intensity	97.0	84.6	89.0	85.6	**86.0**	82.9	**73.5**
Intrinsic features	99.5	90.8	90.6	96.7	**76.5**	87.9	**70.0**

information of 3D images. Here, we compare the recognition performance using the different combination, that is, depth+intensity vs. scattered+associative.

After registration of different 3D images, depth and intensity images are generated. Using AdaBoost learning [22], a strong classifier is constructed based on depth and intensity images. The rank-one recognition accuracy is showed in the first row of Table 3. Another classifier is constructed using intrinsic features by AdaBoost learning (see Section 3). The CCR is showed in the bottom row of Table 3.

From this result, we can see that combination of intrinsic features outperform the combination of depth and intensity in five probe sets. This result suggests that it is a promising way to extract 3D shape information for improving recognition information. Some effective 3D shape features even have better performance than multi-modal 2D+3D. In addition, it is noted that the latter is more robust than the former in large pose variations.

5 Conclusions

Personal identification based on 3D information has recently been gaining more and more interest. We have proposed a novel representation, called associative features, based on Gaussian-Hermite moments, to encode relationships between neighboring mesh nodes. It is integrated by complementary non-relational features to provide an *intrinsic representation* of faces. Then, a powerful learning

algorithm, i.e., AdaBoost, is used for feature selection and classification. One large 3D face database with complex illumination, expression and pose variations has been collected to test the proposed algorithm. The experimental results and the comparisons with some existing methods have demonstrated the excellent performance of the proposed method for 3D face recognition.

Acknowledgment

The authors are grateful to Dr L. Quan for valuable discussions and proofreading this paper. This work is supported by research funds from the Natural Science Foundation of China (Grant No. 60121302 and 60332010), the Outstanding Overseas Chinese Scholars Fund of CAS (Grant No. 2001-2-8), and the National 973 Program (Grant No. 2004CB318100).

References

1. W. Zhao, R. Chellappa, P.J. Phillips, and A. Rosenfeld, "Face Recognition: A Literature Survey", ACM Computing Surveys archive, Vol.35, No.4, pp.399-458, 2003.
2. J.C. Lee, and E. Milios, "Matching Range Images of Human Faces", Proc. ICCV'90, pp.722-726, 1990.
3. G.G. Gordon, "Face Recognition Based on Depth and Curvature Features", Proc. CVPR'92, pp.108-110, 1992.
4. Y. Yacoob and L.S. Davis, "Labeling of Human Face Components from Range Data", CVGIP: Image Understanding, 60(2):168-178, 1994.
5. C.S. Chua, F. Han, and Y.K. Ho, "3D Human Face Recognition Using Point Signiture", Proc. FG'00, pp.233-239, 2000.
6. C. Beumier and M. Acheroy, "Automatic 3D Face Authentication", Image and Vision Computing, 18(4):315-321, 2000.
7. H.T. Tanaka, M. Ikeda and H. Chiaki, "Curvature-based Face Surface Recognition Using Spherical Correlation", Proc. FG'98, pp.372-377, 1998.
8. C. Hesher, A. Srivastava, and G. Erlebacher, "A Novel Technique for Face Recognition Using Range Imaging", Inter. Multiconference in Computer Science, 2002.
9. V. Blanz, and T. Vetter, "Face Recognition Based on Fitting a 3D Morphable Model", IEEE Trans. on PAMI, 25(9):1063-1074, 2003.
10. C. Dorai and A.K. Jain, "COSMOS-A Representation Scheme for 3-D Free-Form Objects", IEEE Trans. on PAMI, 19(10):1115-1130, 1997.
11. X. Lu, D. Colbry, and A.K. Jain, "Three-dimensional Model Based Face Recognition", Proc. ICPR'04, pp.362-365, 2004.
12. M.W. Lee, and S. Ranganath, "Pose-invariant Face Recognition Using a 3D Deformable Model", Pattern Recognition, Vol.36, pp.1835-1846, 2003.
13. Y. Wang, C. Chua, and Y. Ho, "Facial Feature Detection and Face Recognition from 2D and 3D Images", Pattern Recognition Letters, Vol.23, pp.1191-1202, 2002.
14. K.I. Chang, K.W. Bowyer, and P.J. Flynn, "An Evaluation of Multi-model 2D+3D Biometrics", IEEE Trans. on PAMI, 27(4):619-624, 2005.
15. A.M. Bronstein, M.M. Bronstein, and R. Kimmel, "Expression-Invariant 3D Face Recognition", Proc. AVBPA'03, LCNS 2688, pp.62-70, 2003.

16. L.I. Kuncheva, J.C. Bezdek, and R.P.W. Duin, "Decision Templates for Multiple Classifier Fusion: an Experimental Comparon", Patter Recognition, Vol.34, pp.299-314, 2001.
17. C. Xu, Y. Wang, T. Tan, L. Quan, "Automatic 3D Face Recognition Combining Global Geometric Features with Local Shape Variation Information", Proc. FG'04, pp.308-313, 2004.
18. C. Xu, Y. Wang, T. Tan, L. Quan, "Robust Nose Detection in 3D Facial Data Using Local Characteristics", Proc. ICIP'04, pp.1995-1998, 2004.
19. P.J. Phillips, H. Moon, S.A. Rizvi, and P.J. Rauss, "The Feret Evaluation Methodology for Face-Recognition Algorithm", IEEE Trans. on PAMI, 22(10):1090-1104, 2000.
20. J. Shen, W. Shen and D. Shen, "On Geometric and Orthogonal Moments", Inter. Journal of Pattern Recognition and Artificial Intelligence, 14(7):875-894, 2000.
21. P.J. Besl, and N.D. Mckay, "A Method for Registration of 3-D shapes", IEEE Trans. on PAMI, 14(2):239-256, 1992.
22. P. Viola, and M. Jones, "Robust Real-time Object Detection", Proc. 2nd Inter. Workshop on Statistical Computional Theories of Vision, 2001.
23. B. Moghaddam, and A. Pentland, "Beyond Euclidean Eigenspaces: Bayesian Matching for Vision recognition", Face Recognition: From Theories to Applications, ISBN 3-540-64410-5, pp.921, 1998.